Applied Catalysis B: Environmental 83 (2008) 160–167

Contents lists available at ScienceDirect

Applied Catalysis B: Environmental

journal homepage: www.elsevier.com/locate/apcatb

Nanocrystalline beta zeolite: An efficient solid acid catalyst for the liquid-phase degradation of high-density polyethylene

Yun Je Lee [a], Jong-Ho Kim [a], Seok Han Kim [b], Suk Bong Hong [b,*], Gon Seo [a,*]

[a] School of Applied Chemical Engineering and the Center for Functional Nano Fine Chemicals, Chonnam National University, Gwangju 500-757, Republic of Korea
[b] School of Environmental Science and Engineering, POSTECH, Pohang 790-784, Republic of Korea

ARTICLE INFO

Article history:
Received 29 September 2007
Received in revised form 15 February 2008
Accepted 15 February 2008
Available online 23 February 2008

Keywords:
Beta zeolite
Nanocrystallinity
HDPE
Liquid-phase degradation

ABSTRACT

Three pairs of the proton form of beta zeolites with similar Si/Al ratios but notably different crystallite sizes (10–1500 nm) were prepared in basic or fluoride media and tested as catalysts for the liquid-phase degradation of high-density polyethylene at 380 °C and atmospheric pressure. Among these, a nanocrystalline beta zeolite with the lowest Si/Al ratio (10.7) and the smallest crystallite size (~10 nm) was found to show a high degradation activity and a remarkable liquid products yield (~80%), together with high selectivities for C_7–C_{12} hydrocarbons, which is rationalized on the basis of its very large external surface area and its high acidity compared to the other beta zeolites studied here.

1. Introduction

Polymeric materials are widely used in industry and home because of their convenience and low price. While the production size of such materials is very large, the life span of packing materials, agricultural films, electric and electronic devices, etc., are not so long, resulting in a huge amount of post-use waste polymers that are mostly landfilled or incinerated. However, these disposal methods tend to be prohibited due to possible soil and air pollution. Consequently, there is a strong incentive to develop an efficient way to recycle polymeric materials with no secondary pollutants generated [1–20], because waste polyethylene can be converted to lower hydrocarbons, capable of using as fuels, through the degradation reaction. Its thermal degradation is quite simple in terms of process operation, but is energy-intensive. Due to the very broad distribution of degraded products obtained in this way, furthermore, much attention has been devoted to the search for catalysts which could lower notably the degradation temperature of polyethylene, while giving the enhanced yield in liquid products that are more convenient than gas fuels in the aspects of handling and storage.

Aluminosilicate zeolites, an important class of microporous materials, have been repeatedly shown to be promising solid acid catalysts for the degradation of polyethylene over the past decade [1–18]. Clearly, polyethylene is too large to enter into the zeolite micropores. So it degrades initially over the acid sites located on the external surface of zeolite crystals. Then, the initially cracked fragments can diffuse through the zeolite pores and react further, to produce lower hydrocarbons. This implies that a zeolite with a smaller crystallite size should be better for the catalytic degradation of polyethylene due to its larger external surface [1–4,17]. To be an efficient degradation catalyst, in addition, the zeolite should possess a reasonable amount of strong acid sites, because polyethylene degrades on acid sites. However, the presence of so many such acid sites results in severe formation of coke deposits inside the pores of zeolite crystals, as well as on their external surface, followed by rapid catalyst deactivation [12,14]. Therefore, the acidity and crystallite size of zeolites are two important factors determining their activity and selectivity during the catalytic degradation of polyethylene.

Various zeolites and mesoporous materials have been employed in the catalytic degradation of polyethylene such as H-ZSM-5, H-beta, H-Y, SAPO-37, AlMCM-41 and AlTUD-1 [1–24]. These catalysts show different activity according to their pore structure, acidity and crystallite size. Their activities are very important in determining the required amount of catalysts for the complete conversion of polyethylene in its catalytic degradation. However, it is difficult to evaluate the activity of catalysts in the catalytic degradation because the reaction conditions including reactor types, test modes, polymer/catalyst ratios, temperature profiles and operation methods strongly influence their activity

* Corresponding author.
E-mail addresses: sbhong@postech.ac.kr (S.B. Hong), gseo@chonnam.ac.kr (G. Seo).

0926-3373/$ – see front matter © 2008 Elsevier B.V. All rights reserved.
doi:10.1016/j.apcatb.2008.02.013

[25,26]. The simultaneously proceeding of various reactions of melted polyethylene molecules over catalysts in the liquid-phase degradation such as cracking, oilgomerization, isomerization, hydride transfer, and carbon deposit brings about different activity orders of catalysts according to the test methods because the rates of the reactions change differently with the reaction conditions. The structure of polyethylene also affects on the rate of its catalytic degradation [27,28].

H-ZSM-5 with an intersecting 10-ring pore system between the straight (5.3 × 5.6 Å) and the sinusoidal (5.1 × 5.5 Å) channels is one of the most active catalyst tested for the degradation reaction [1–5]. Its unique three-dimensional pore topology is known to effectively prevent the formation of large hydrocarbon molecules that can be subsequently converted to coke. A distinguishing feature of this medium-pore zeolite is a high cracking activity for the initially cracked fragments inside the 10-ring channels, producing small gaseous hydrocarbons mainly composed of C_2–C_6 hydrocarbons. Thus, the liquid products yield over H-ZSM-5 is usually below 50%, revealing that the pore size of zeolites is acting as an important product selectivity factor in the polyethylene degradation.

Beta zeolite is a large-pore material with mutually perpendicular intersecting 12-ring (5.6 × 5.6 and 6.6 × 6.7 Å) channels [29]. Recently, several papers reported the high liquid products yield in the degradation of polyethylene over H-beta compared to H-ZSM-5, mainly due to the larger pore size of the former zeolite compared to the latter one, leading to a less extent of the subsequent cracking [13,16–18]. The comparable activity of H-beta zeolites to H-ZSM-5 zeolites in the catalytic degradation is usually explained by its large pore diameter, high acidity, and large external surface area. The effect of crystallite size of beta zeolites on their activity in the catalytic degradation of polyethylene was reported [16]. The small-sized beta zeolite (100 nm) showed better activity than large-sized one (12,000 nm), even though the effect of acidity on the catalytic activity of beta zeolites was not concerned. Therefore, nanocrystalline beta zeolites with sufficient acidity are expected to be efficient catalysts to achieve high conversions as well as high liquid products yields in the liquid-phase degradation of polyethylene.

Here we have prepared three pairs of the proton form of beta zeolites with similar bulk Si/Al ratios (10–50) but significantly different crystallite sizes (10–1500 nm) and compared their catalytic properties for the liquid-phase degradation of high-density polyethylene (HDPE), to gain a better understanding of the effects of their crystal size and acidity on the HDPE conversion and product distribution.

2. Experimental

2.1. Catalyst preparation

Six beta zeolites with different Si/Al ratios or crystallite sizes were synthesized using tetraethylammonium hydroxide (TEAOH, 35 wt% solution in water, Aldrich) as an organic structure-directing agent (SDA) in basic or fluoride media [30,31]. The detailed preparation conditions for all beta materials employed here are given in Table 1. The solid products obtained in basic media were recovered by centrifugation (12,000 rpm, 60 min) followed by redispersion in deionized water, three times in total, and those in fluoride media were separated by filtration, washed repeatedly with water and dried overnight at room temperature. The proton form of each beta sample was prepared by calcining its as-made form in air at 550 °C for 20 h. For comparison, H-ZSM-5 with a Si/Al ratio of 25 and an average crystallite size of ca. 100 nm was obtained from Zeolyst.

2.2. Characterization

Powder X-ray diffraction (XRD) patterns were collected on a Rigaku Miniflex diffractometer with Cu K_α radiation. Elemental analysis was carried out by a Jarrell-Ash Polyscan 61E inductively coupled plasma spectrometer in combination with a Perkin–Elmer 5000 atomic absorption spectrophotometer. Crystallite size was determined by a Hitachi S-4700 scanning electron microscope (SEM) or a JEOL 2000FX II transmission electron microscope (TEM). The N_2 sorption experiments were performed on a Mirea SI Nanoporosity-PQ analyzer. Temperature-programmed desorption (TPD) of ammonia was recorded on a fixed-bed, flow-type apparatus attached to a Balzers TCP 015 quadrupole mass spectrometer. Before adsorption of ammonia, 0.1 g of sample were pretreated in flowing He (100 $cm^3\ min^{-1}$) at 550 °C for 2 h. Then, ammonia pulses were injected to the sample at 150 °C until saturated. The treated sample was subsequently purged with He at the same temperature for 1 h to remove the physisorbed ammonia. Finally, TPD profiles were obtained in flowing He from 150 to 600 °C with a ramping rate of 10 °C min^{-1}.

Table 1
Synthesis conditions and characterization data for beta zeolites with different Si/Al ratios or crystallite sizes employed in this study[a]

Catalyst	Gel composition[b]	t (days)	Si/Al ratio		Average crystallite size[d] (nm)	BET surface area[e] ($m^2\ g^{-1}$)	Micropore volume[f] ($cm^3\ g^{-1}$)	Mesopore volume[g] ($cm^3\ g^{-1}$)
			In gel	In zeolite[c]				
Beta-AI	48.0TEAOH•3.2Al_2O_3•80SiO_2•1200H_2O	10	12.5	10.7	10	621	0.12	0.83
Beta-AII	43.2TEAOH•0.8Al_2O_3•80SiO_2•1200H_2O	6	50	26	40	580	0.16	0.43
Beta-AIII	42.0TEAOH•0.2Al_2O_3•80SiO_2•1200H_2O	6	200	52	150	465	0.16	0.14
Beta-BI	49.6TEAOH•49.6HF•3.2Al_2O_3•80SiO_2•726.4H_2O	14	12.5	12.9	>500	488	0.18	0.01
Beta-BII	46.4TEAOH•46.4HF•1.6Al_2O_3•80SiO_2•723.2H_2O	6	25	27	1000	395	0.14	0.01
Beta-BIII	44.8TEAOH•44.8HF•0.8Al_2O_3•80SiO_2•721.6H_2O	6	50	56	1500	524	0.18	0.01
H-ZSM-5[h]				25	100	413	0.12	0.07

[a] Crystallization was performed with stirring (60 rpm) at 140 °C. Prior to the crystallization, the final synthesis mixture was aged with stirring at room temperature for 1 day.
[b] Fumed silica (Aerosil 200, Degussa) and tetraethylorthosilicate (TEOS, 98%, Aldrich) were used as the SiO_2 starting material for the former three and latter three beta samples, respectively. The other reagents included tetraammonium hydroxide (TEAOH, 35 wt% solution in water, Aldrich), Al metal powder (99.5%, Wako), and hydrofluoric acid (HF, 50 wt% solution in water, Duksan).
[c] Determined from elemental analysis.
[d] Estimated from TEM or SEM mesurements.
[e] Calculated from N_2 adsorption data of the proton form of each zeolite.
[f] In the diameter range ≤20 Å.
[g] In the diameter range 20–500 Å. Calculated using the BJH formalism.
[h] Obtained from zeolyst.

2.3. Liquid-phase HPDE degradation

The liquid-phase degradation of HDPE over zeolite catalysts was carried out in a batch reactor described in our previous paper [19,30]. Typically, 10 g of HDPE (Honam Petrochem.) with an average molecule weight of 280,000 and 0.03 or 0.1 g of zeolite catalyst were charged into a 100 ml round-bottomed flask and purged with N_2 flow (45 cm^3 min^{-1}) to remove oxygen. Since the thermal degradation of HDPE used in this study was initiated above 400 °C, the reaction temperature was fixed to 380 °C, to avoid the thermal degradation of HDPE. Liquid products were collected in a burette through a condenser maintained at −4 °C. The amount of gaseous products was determined by measuring continuously the product flow using a Ritter TG05 gas flow meter. The reaction products were analyzed on-line using a Donam DS 6200 gas chromatograph equipped with a HP-1 capillary column (0.32 mm × 50 m) and a flame ionization detector. A standard kit of *n*-paraffins (Fisher, US-ASTM-100) was employed in attempts to assign the peaks of liquid products in the C_5–C_{20} range.

Conversion was defined as the percentage of HDPE converted to gas and liquid products in the liquid-phase degradation. The amount of HDPE degraded was calculated from the change in weight of the round-bottomed flask before and after the reaction. The liquid products yields were determined from the amount of liquid collected in the burette and the gas products yields were obtained from the difference between the conversion and liquid products yield. The gas products yield obtained was confirmed by the amount of gas products determined by integrating them through the degradation reaction. Since the main components of the gas products were propylene and butenes, their composition were assumed to be equimolar mixtures of propylene and butane for the calculation of gas products yields.

3. Results and discussion

3.1. Physico-chemical properties of beta zeolites

Fig. 1 shows the powder XRD patterns of the proton form of all six beta zeolites employed in this study. No diffractions other than those from beta zeolite are observed. However, most of the X-ray peaks from the three beta zeolites synthesized in basic media are significantly broader than those from the three beta zeolites prepared in fluoride media with similar bulk Si/Al ratios, respectively, as previously reported [31,32]. This is a consequence of the considerably smaller crystallite size of the former three beta zeolites (see below) and not an indication of their poorer crystallinity, because the areas under peaks remain nearly similar for all cases. Fig. 1 also shows that in the case of beta zeolites obtained in basic media (i.e., beta-AI, beta-AII, and beta-AIII), there is a noticeable broadening and a decrease in the heights of all the X-ray peaks as Si/Al ratio of the zeolite decreases (Table 1). This suggests that the beta-AI zeolite with the lowest Si/Al ratio (10.7) has the smallest crystallite size among the beta zeolites studied here (see below).

Fig. 2 shows the SEM images of the three beta zeolites prepared in basic media, together with those of the beta zeolites synthesized in fluoride media, and Fig. 3 shows their TEM images. These data reveal a large increase in the crystallite size of the beta zeolites as their Si/Al ratio of the beta zeolite increases from 10.7 to 52 (Table 1), while all zeolites obtained in basic media are clearly nanocrystalline. The beta-AI sample was found to have the smallest crystallite size (∼10 nm). Unlike the beta-AIII zeolite with the relatively well-defined crystallite size (∼150 nm), however, the beta-AI and beta-AII samples tend to aggregate, making difficult to determine their morphology. As seen in Fig. 2, on the other hand, all beta zeolites obtained in fluoride media are, in principle, microcrystalline and are characterized by the well-faceted, truncated square bipyramidal morphology, typical of this zeolite. Therefore, it is clear that for crystalline solids with similar Si/Al ratios, the crystals synthesized in fluoride media are much bigger than those prepared in basic media, which is consistent with the trend observed in previous studies [31,32].

Table 1 lists the bulk Si/Al ratio and average crystallite size of all beta zeolites studied here. There is a trend of decreasing the Si/Al ratio of beta zeolites synthesized in basic media with increasing the ratio of their synthesis mixtures. However, the Si/Al ratio of each material crystallized in fluoride media is quite similar to the ratio of its synthesis mixture. By adjusting the Si/Al ratio of their

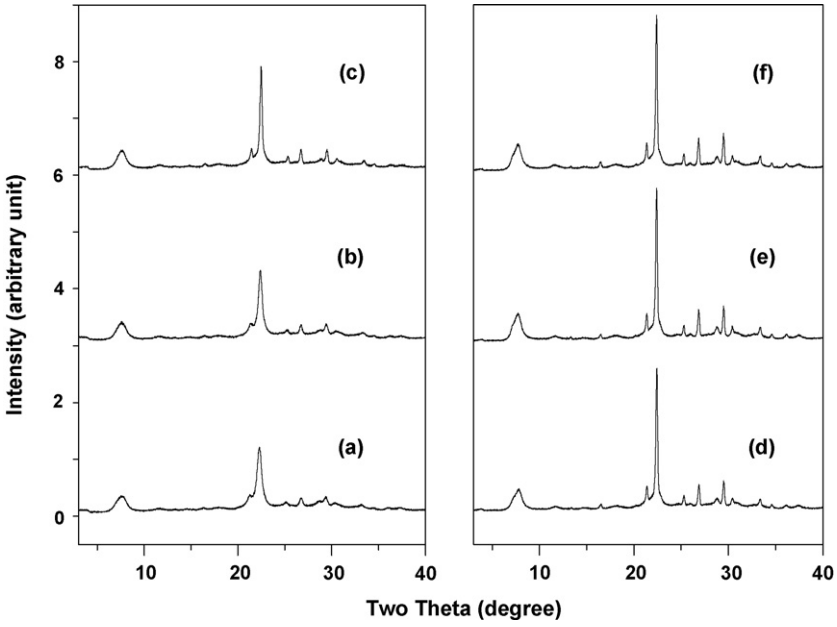

Fig. 1. Powder XRD patterns of the proton form of (a) beta-AI, (b) beta-AII, (c) beta-AIII, (d) beta-BI, (e) beta-BII, and (f) beta-BIII zeolites.

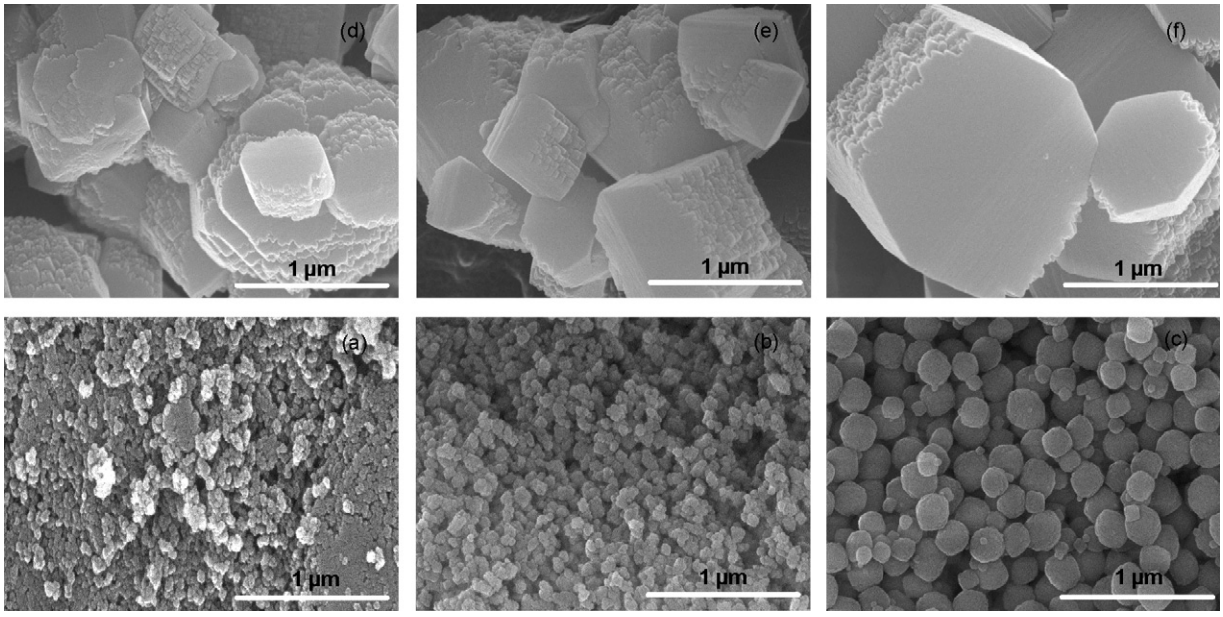

Fig. 2. SEM images of as-made (a) beta-AI, (b) beta-AII, (c) beta-AIII, (d) beta-BI, (e) beta-BII, and (f) beta-BIII zeolites.

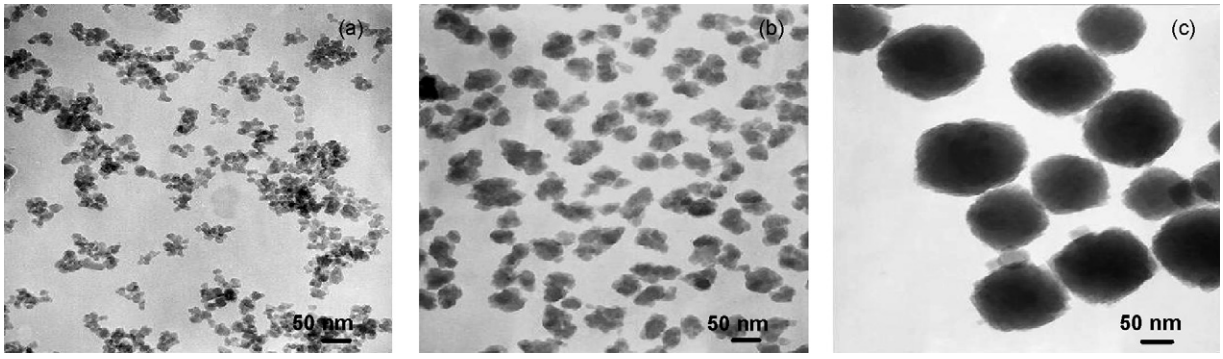

Fig. 3. TEM images of the three beta zeolites prepared in basic media: (a) beta-AI, (b) beta-AII, and (c) beta-AIII.

synthetic mixture based on these results, three pairs of beta zeolites with similar Si/Al ratios have been successfully prepared by using different mineralizing agents (i.e., OH^- and F^-).

Fig. 4 shows the N_2 adsorption–desorption isotherms of the proton form beta zeolites. The isotherms of the beta zeolites are considerably different according to their crystallite size in the aspects of hysteresis. Nanocrystalline beta-A zeolites have small hysteresis loops. A hysteresis loop observed on the isotherm of the beta-AI is clear around $P/P_o = 0.9$, while that of the beta-AIII is very weak. The microcrystalline beta-B zeolites do not show any hysteresis. The slopes of the isotherms of the beta-AI and -AII increase gradually with the relative pressure of nitrogen. However, the isotherms of the microcrystalline beta-B zeolites are typical Langmuir ones without showing any increase in the slopes of their isotherms. The observation of the hysteresis and the increases in the slopes from the isotherms of the beta-AI and -AII indicate that these beta zeolites are composed of extremely small crystallites which are from mesopores among them [17].

The surface areas and pore volumes of beta zeolites obtained from their N_2 sorption isotherms are also listed in Table 1. BET surface areas of the beta-AI and -AII are very high about 600 $m^2\,g^{-1}$, while those of others are in the range of 400–500 $m^2\,g^{-1}$. The more clear difference is observed from their mesopore volumes. Nanocrystalline beta zeolites exhibit notably large mesopore volumes, which is more apparent to the materials with lower Si/Al ratios. For example, the mesopore volumes of the H-beta-AI and H-beta-BI were determined to be 0.83 and 0.01 $cm^3\,g^{-1}$, respectively. This is not unexpected because the crystallite size (~10 nm) of the former zeolite is much smaller than that (>500 nm) of the latter zeolite (Figs. 1 and 2).

Fig. 5 compares the NH_3 TPD profiles from three pairs of beta zeolites with similar bulk Si/Al ratios but notably different crystallite sizes. In general, the lower Si/Al ratio the zeolite has, the larger area of desorption peak it shows. However, no significant differences in the temperature maximum of desorption peak were found, despite large differences in the crystallite size. This suggests that the crystallite size effect on the acidic properties of H-beta zeolites is negligible. If such were the case, the catalytic results obtained from three pairs of beta zeolites with similar bulk Si/Al ratios but different crystallite sizes could then illustrate the effects of zeolite crystallite size rather than those of acidity on their HDPE degradation activities. It should be noted here that the temperature maximum (~320 °C) of NH_3 desorption peak from any of our H-beta zeolites is considerably lower than that (~410 °C) from H-ZSM-5 with Si/Al = 25 that will be used as a reference catalyst below. This indicates that the strong acid sites in H-beta zeolites

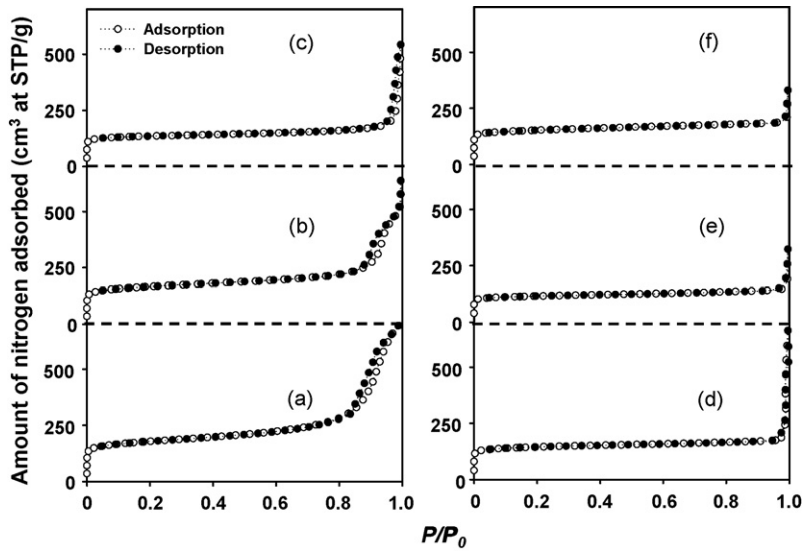

Fig. 4. Adsorption and desorption isotherms of nitrogen on (a) beta-AI, (b) beta-AII, (c) beta-AIII, (d) beta-BI, (e) beta-BII, and (f) beta-BIII at liquid nitrogen temperature.

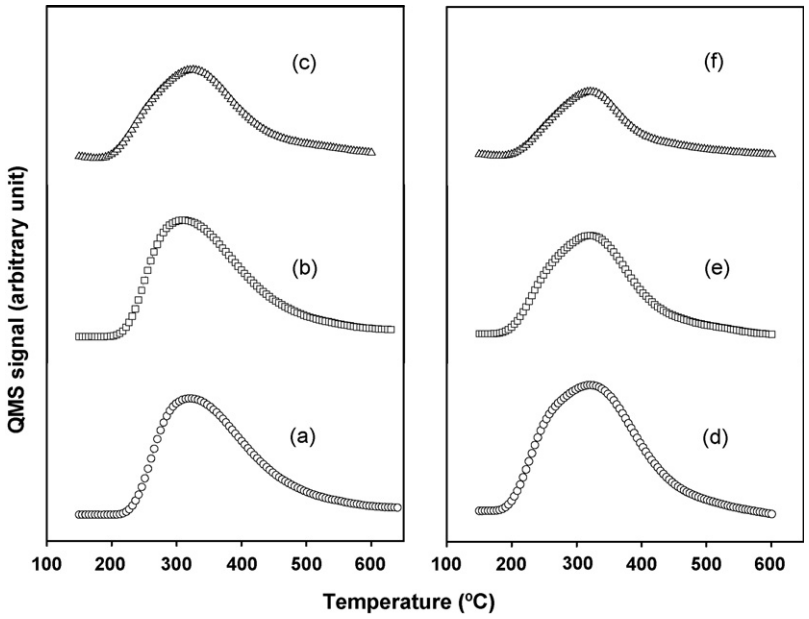

Fig. 5. NH_3 TPD profiles from (a) H-beta-AI, (b) H-beta-AII, (c) H-beta-AIII, (d) H-beta-BI, (e) H-beta-BII, and (f) H-beta-BIII zeolites.

possess a lower strength than those in H-ZSM-5, as repeatedly shown [19,33].

3.2. Liquid-phase degradation of HDPE

Since the catalytic liquid-phase degradation of HDPE produces various hydrocarbons with different molecular weights, we checked the mass balance of the catalytic degradation. Table 2 lists the conversions and yields of the catalytic degradation over various zeolites at 380 °C. The conversions were determined from the weight loss of the reactor contained HDPE and catalyst due to the degradation reaction. The products yields of gas and liquid were calculated from the integrated amount of gas products and the collected amount of liquid products, respectively. However, six catalysts except the H-beta-BIII show small differences between the conversions and the summed yields of gas and liquid products, about 1% or less. These small differences mean that the gas and liquid products obtained satisfactory reflect the degradation reaction.

Fig. 6 shows HDPE conversion as a function of time on stream in the liquid-phase degradation of HDPE over three pairs of H-beta zeolites with similar Si/Al ratios but different crystallite sizes at 380 °C and atmospheric pressure. For comparison, the catalytic results from H-ZSM-5 with Si/Al = 25 and crystallite size ~100 nm, which is thus nanocrystalline in nature, are also given in Fig. 6. The temperature profile presented as dotted line, shows that about 10 min are required to reach the reaction temperature up to 380 °C. Among the H-beta zeolites studied here, the degradation rate over nanocrystalline H-beta-AI and H-beta-AII with crystallite sizes <50 nm at an HDPE/catalyst ratio of 10 g/0.1 g was found to be comparable to that of H-ZSM-5 known as an active catalyst for this reaction. In contrast, the lowest degradation activity is observed for H-beta-AIII with a larger crystallite (~150 nm) and a higher Si/Al ratio (52). Fig. 6 also shows that microcrystalline H-beta-BI and

Table 2
Conversions and products yields in the catalytic degradation of HDPE at 380 °C for 80 min

Catalyst	Conversion[a] (%)	Yield (%)		Difference[d] (%)
		Liquid[b]	Gas[c]	
Beta-AI	96	78	19	1
Beta-AII	98	77	20	1
Beta-AIII	8	–	7	1
Beta-BI	60	42	18	0
Beta-BII	10	3	7	0
Beta-BIII	26	10	10	6
H-ZSM-5	99	62	37	0

[a] Calculated from the weight loss of reactor before and after the degradation.
[b] Calculated from the liquid products collected in the buret.
[c] Calculated from the integrated amount of gas produced in the degradation using the ideal gas equation.
[d] Difference between the conversion and the sum of gas and liquid products yields.

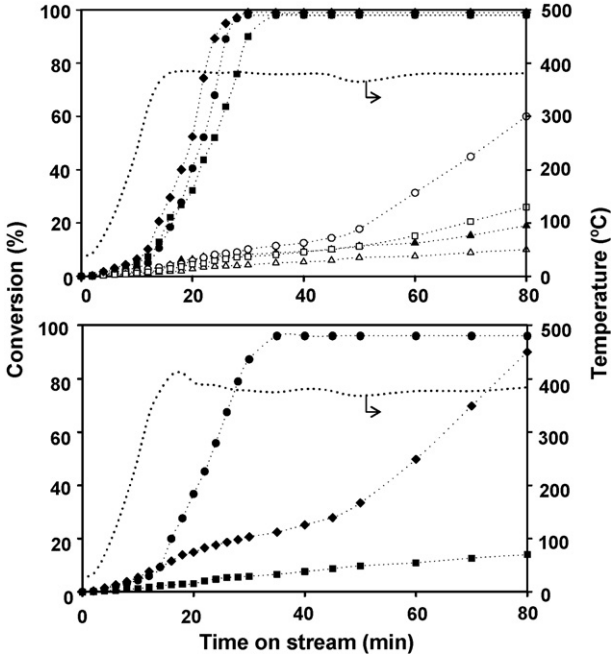

Fig. 6. HDPE conversion as a function of time on stream in liquid-phase HDPE degradation over H-beta-AI (●), H-beta-AII (■), H-beta-AIII (▲), H-beta-BI (○), H-beta-BII (□), H-beta-BIII (△), and H-ZSM-5 (◆) at 380 °C, HDPE/catalyst = 10 g/0.1 g (up) and 10 g/0.03 g (down), and atmospheric pressure.

H-beta-BII with similar Si/Al ratios to those of nanocrystalline H-beta-AI and H-beta-AII, respectively (Table 1), are characterized by much lower degradation activities. Therefore, it is clear that the crystallite size of H-beta zeolites rather than their Si/Al ratio is a critical factor affecting the HDPE degradation activity [16].

The low activity of H-beta-AIII is unexpected because it is a nanocrystalline beta zeolite. However, its external surface area deduced from its mesopore volume is considerably small compared to the H-beta-AI and H-beta-AII (Table 1). Its acidity is also lower than the H-beta-BI and -BII due to its high Si/Al ratio. Therefore, the insufficient large external surface area and low acidity of the H-beta-AIII may cause its poor activity in the catalytic degradation of HDPE.

To more accurately examine the HDPE degradation activities over the H-beta-AI, H-beta-AII, and H-ZSM-5, we have reduced the catalyst amount from 0.1 to 0.03 g and performed the degradation reaction under the identical conditions as those described above. It is nearly impossible to reuse the catalysts used in the liquid-phase degradation because of carbon deposit and contamination by soil on them at the practical catalytic degradation of waste polyethylene. The reduction of the catalyst amount required for the complete degradation, therefore, is very important to improve the economic feasibility of the catalytic degradation. As seen in Fig. 6, the H-beta-AI with the smallest crystallite size (~10 nm) and the lowest Si/Al ratio (~10) among the H-beta zeolites prepared in our work, is much more active than the H-beta-AII and H-ZSM-5. The reduction of the catalyst amount leads the slow degradation over the H-beta-AII and H-ZSM-5, but the degradation over the H-beta-AI is still rapid even with 0.03 g of it. It is also remarkable that a much larger catalyst amount (HDPE/catalyst = 10 g/0.2 g) was necessary to achieve almost 100% conversion, when the commercially available H-beta zeolite with a similar Si/Al ratio (12.5) to that (10.7) of the H-beta-AI zeolite is used as a catalyst under the identical reaction conditions [19].

The increase of the conversion rate with time on stream varies with the catalysts employed. The active catalysts, H-beta-AI and H-beta-AII, show rapid increases of the conversion as shown in the upper part of Fig. 6, while the increasing rates of the conversion over the low active catalysts, H-beta-BII and H-beta-BIII, are very slow. However, the H-beta-BI shows considerably different behavior: the conversion rate increases remarkably after around 50 min when the amount of the catalysts loaded is 0.1 g per 10 g of HDPE. Similar behavior appears over the H-ZSM-5 after around 30 min when its loading is 0.03 g. These time lags for the remarkable increases of the conversion rate are usually observed on the catalysts with small number of acid sites due to their small catalyst loading or their inherent low density of acid sites. Many catalytic cracking steps for the degradation of polymer molecules to small molecules to be collected as gas and liquid products are responsible for the time lag. The slope change of the conversion rate reflects the reaction time requiring for the accumulation of cracked fragments on the catalysts. Their further cracking in the pores of the catalysts causes the appreciable production of gas and liquid products, resulting in the remarkable increase of the conversion rate. The catalysts with sufficient amount of acid sites do not induce the time lag because of the rapid degradation over them, while the catalysts with low activity also do not show the time lag due to their extremely slow progress of the degradation.

To date, there are several comparative studies on the catalytic degradation of polyethylene over various zeolites [1,2,7–13]. However, it is not easy to compare their activities from the reported results because the reaction conditions and test modes were not the same. Since the degradation rate of polyethylene proceeds through complicated reaction paths, even the difference in temperature mode, i.e. constant or programmed, results different activity order of the catalysts. The temperature itself also influences the rate of catalytic degradation because the radicals formed through thermal degradation of polyethylene at elevated temperatures contribute to the catalytic degradation. However, H-ZSM-5 and H-beta zeolites are generally considered to be active in the liquid-phase degradation of HDPE when its thermal degradation does not occur [1,17,18]. The strong acidity and particular sinusoidal pores of H-ZSM-5 result in rapid degradation of polyethylene over it, unless its crystallite size is too large [34]. On the other hand, three-dimensionally connected large pores of H-beta zeolites enhance the liquid products yield, while their weak acidic property leads usually slow degradation rate compared to H-ZSM-5 [19].

However, the H-beta-AI shows higher activity than the H-ZSM-5 in the catalytic degradation of HDPE when the amount of the catalyst loaded is as small as 0.03 g per 10 g of HDPE, as shown in Fig. 6. The degradation of HDPE on zeolite catalysts proceeds

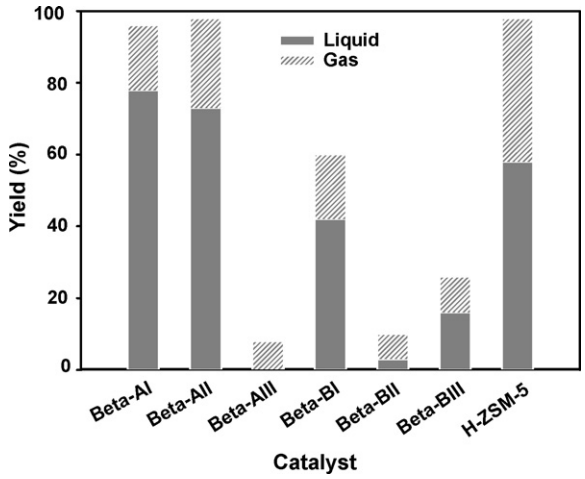

Fig. 7. Gas and liquid products yields in HDPE degradation over three pairs of H-beta zeolites with similar Si/Al ratios but different crystallite sizes recorded after 60 min on stream at 380 °C and HDPE/catalyst = 10 g/0.1 g. The catalytic data from H-ZSM-5 zeolite with Si/Al = 25 are included for comparison.

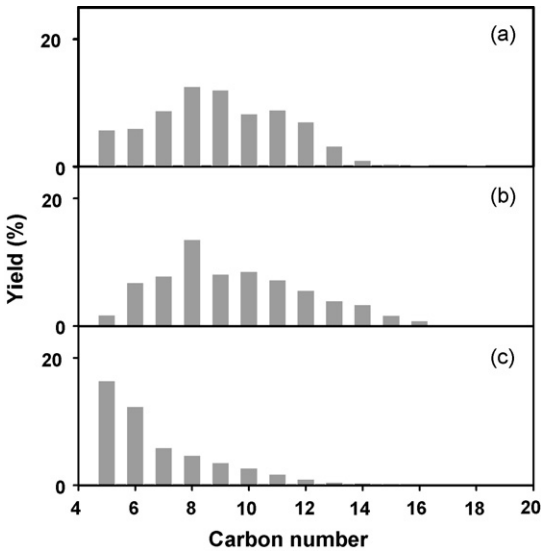

Fig. 8. Liquid products distribution from liquid-phase HDPE degradation over (a) H-beta-AI, (b) H-beta-AII, and (c) H-ZSM-5 at 380 °C and HDPE/catalyst = 10 g/0.1 g. Reported as the value of 60 min on stream.

through several consecutive reactions: the cracking at the pore entrance and on the external surface of zeolites and further cracking in their pores. When the amount of the catalyst loaded is small, the acid sites located at pore entrances and on the external surface for the initiation of catalytic cracking are insufficient. Therefore, the catalytic cracking on the external surface is more important than the further cracking in the pores, resulting in rapid degradation of HDPE on the H-beta-AI with large external surface area. On the other hand, the activity for the further cracking in the pores of zeolites determines the degradation rate when the amount of catalyst loaded is sufficient for the initial cracking of HDPE on the external surface. Since the acidity of H-ZSM-5 zeolite is stronger than that of H-beta zeolite as described above, the H-ZSM-5 shows higher activity than the H-beta-AI when the catalyst loading is 0.10 g.

Fig. 7 shows gas and liquid products yields in the HDPE degradation over all zeolite catalysts studied, which were measured after 60 min on stream at 380 °C and HDPE/catalyst = 10 g/0.1 g. It can be seen that at HDPE conversion levels >95% the H-beta-AI is considerably selective for the formation of liquid products compared to the H-ZSM-5 (80 vs. 60%), which is also the case of the H-beta-AII with a slightly larger crystallite size (~40 nm). The liquid products yield in the HDPE degradation can differ according to the pore structure of catalysts used. The beta zeolite with large pores causes the high yield of liquid products as suggested on Y zeolites and Al-containing mesoporous material [8,10,22,24].

The carbon number distributions of liquid products from the catalytic degradation of HDPE over the two nanocrystalline H-beta zeolites in the conditions described above, together with H-ZSM-5, are compared in Fig. 8. Notice that the distributions of the liquid products obtained over the nanocrystalline H-beta-AI and -AII zeolites are spread from C_5 to C_{13} hydrocarbons. We also note that the distribution patterns are nearly symmetric at a maximum of C_8 or C_9 hydrocarbons. However, H-ZSM-5 shows the highest fraction in C_5 hydrocarbons, which is in good agreement with the trend reported in previous studies [16,19,30,35]. The lower acidity, larger pore diameter and smaller crystallite size of the nanocrystalline beta zeolites reduce further cracking in their pores, resulting in the preservations of larger hydrocarbons compared to H-ZSM-5.

Apparently, nanocrystalline H-beta zeolites have considerably larger external surface areas than microcrystalline ones (Table 1), which should be responsible for their higher rate of HDPE degradation. As described above, on the other hand, the pore size of zeolites is an important factor determining the yield and product distribution from the degradation reaction over this class of solid acids, due to the diffusion of the initially cracked fragments over the acid sites located on the external surface of zeolite crystallites into their pores in which the subsequent cracking to lower hydrocarbons should occur. Beta zeolite has a three-dimensional, 12-ring pore system. Thus, it can be expected that the mass transfer in this large-pore material should be faster than that in the medium-pore ZSM-5 zeolite, which is more evident to nanocrystalline materials with a shorter diffusion path. Furthermore, the acid strength of the former zeolite is generally weaker than the latter zeolite [30,33]. On the basis of these arguments, therefore, we conclude that cracking of the initially cracked products inside the beta zeolites pores can be effectively suppressed, leading to a remarkable liquid products yield, along with high selectivities for C_7–C_{12} hydrocarbons, as observed with H-beta-AI and H-beta-AII (Figs. 7 and 8).

4. Conclusions

Nanocrystalline H-beta zeolite with a crystallite size of ~10 nm and low Si/Al ratio was found to be an efficient catalyst in the liquid-phase degradation of HDPE, producing a large amount of liquid products that are suitable as fuels. HDPE of 10 g could be completely converted to lower hydrocarbons even with 0.03 g of the nanocrystalline H-beta zeolite at 380 °C. Both the crystallite size and acidity of H-beta zeolites are important factors influencing their catalytic activity and product distribution. The high activity and high liquids yield of nanocrystalline beta zeolites can be rationalized by considering the rapid cracking of HDPE over the strong acid sites on the external surface and fast mass transfer of cracked fragments in the pores of nanocrystalline H-beta zeolite. The decreased intracrystalline residence time of cracked fragments leads to less cracking reactions, resulting in high liquid products yield.

Acknowledgements

Financial support of this work was provided by the center for Functional Nano Fine Chemicals of Chonnam National University

and by the National Research Laboratory Program (R0A-2007-000-20050-0) of the Korea Science and Engineering Foundation.

References

[1] J. Aguado, D.P. Serrano, G. San Miguel, J.M. Escola, J.M. Rodriguez, J. Anal. Appl. Pyrol. 78 (2007) 153.
[2] D.P. Serrano, J. Aguado, J.M. Rodriguez, A. Peral, J. Anal. Appl. Pyrol. 79 (2007) 456.
[3] J.F. Mastral, C. Berrueco, M. Gea, J. Ceamanos, Polym. Degrad. Stab. 91 (2006) 3330.
[4] D.P. Serrano, J. Aguado, J.M. Escola, J.M. Rodriguez, J. Anal. Appl. Pyrol. 74 (2005) 353.
[5] Ma del Remedio Hernandez, A.N. Garcia, A. Marcilla, J. Anal. Appl. Pyrol. 78 (2007) 272.
[6] Y.-H. Lin, M.-H. Yang, Appl. Catal. A 328 (2007) 132.
[7] J.-R. Kim, J.-H. Van, D.-W. Park, M.-H. Lee, React. Kinet. Catal. Lett. 81 (2004) 73.
[8] A. Marcilla, A. Gomez-Siurana, F.J. Valdes, Microporous Mesoporous Mater. 103 (2008) 420.
[9] S. Ali, A.A. Garforth, D.H. Harris, D.J. Rawlence, Y. Uemichi, Catal. Today 75 (2002) 247.
[10] Ma del Remedio Hernandez, A.N. Garcia, A. Gomez, J. Agullo, A. Marcilla, Ind. Eng. Chem. Res. 45 (2006) 8770.
[11] K. Gobin, G. Manos, Polym. Degrad. Stab. 83 (2004) 267.
[12] Y.S. You, J.-S. Shim, J.-H. Kim, G. Seo, Catal. Lett. 59 (1999) 221.
[13] J. Agullo, N. Kumar, D. Berenguer, D. Kubicka, A. Marcilla, A. Gomez, T. Salmi, D.Yu. Murzin, Kinet. Catal. 48 (2007) 535.
[14] A. Marcilla, M.I. Beltran, A. Gomez-Siurana, R. Navarro, F. Valdes, Appl. Catal. A 328 (2007) 124.
[15] A. Marcilla, A. Gomez-Siurana, D. Berenguer, Appl. Catal. A 301 (2006) 222.
[16] J. Aguado, D.P. Serrano, J.M. Escola, E. Garagorri, J.A. Fernandez, Polym. Degrad. Stab. 69 (2000) 11.
[17] A. Marcilla, A. Gomez-Siurana, F. Valdes, J. Anal. Appl. Pyrol. 79 (2007) 433.
[18] A. Marcilla, A. Gomez-Siurana, F. Valdes, Polym. Degrad. Stab. 92 (2007) 197.
[19] J.W. Park, J.-H. Kim, G. Seo, Polym. Degrad. Stab. 76 (2002) 495.
[20] L.B. Pierella, S. Renzini, O.A. Anunziata, Microporous Mesoporous Mater. 81 (2005) 155.
[21] R.A. Garcia, D.P. Serrano, D. Otero, J. Anal. Appl. Pyrol. 74 (2005) 379.
[22] I.C. Neves, G. Botelho, A.V. Machado, P. Rebelo, S. Ramoa, M.F.R. Pereira, A. Ramanathan, P. Pescarmona, Polym. Degrad. Stab. 92 (2007) 1513.
[23] G.J.T. Fernandes, V.J. Fernandes Jr., A.S. Araujo, Catal. Today 75 (2002) 233.
[24] Y.-H. Lin, M.-H. Yang, T.-F. Yeh, M.-D. Ger, Polym. Degrad. Stab. 86 (2004) 121.
[25] N.S. Akpanudoh, K. Gobin, G. Manos, J. Mol. Catal. A 235 (2005) 67.
[26] K.-H. Lee, D.-H. Shin, Y.-H. Seo, Polym. Degrad. Stab. 84 (2004) 123.
[27] A. Marcilla, M.I. Beltran, F. Hernandez, R. Navarro, Appl. Catal. A 278 (2004) 37.
[28] A. Marcilla, M.I. Beltran, R. Navarro, Appl. Catal. A 333 (2007) 57.
[29] International Zeolite Association, Structure Commission, http://www.iza-structure.org.
[30] J.-S. Shim, Y.S. You, J.-H. Kim, G. Seo, Stud. Surf. Sci. Catal. 121 (1999) 465.
[31] M.A. Camblor, A. Corma, A. Mifsud, J. Perez-Pariente, S. Valencia, Stud. Surf. Sci. Catal. 105 (1997) 341.
[32] M.A. Camblor, A. Corma, S. Valencia, J. Mater. Chem. 8 (1998) 2137.
[33] N. Katada, H. Igi, J.-H. Kim, M. Niwa, J. Phys. Chem. B 101 (1997) 5969.
[34] Y.S. You, J.-H. Kim, G. Seo, Polym. Degrad. Stab. 70 (2000) 365.
[35] D.P. Serrano, J. Aguado, J.M. Escola, E. Garagorri, J.M. Rodriguez, L. Morselli, G. Palazzi, R. Orsi, Appl. Catal. B 49 (2004) 257.